Journal of Catalysis **203,** 434–442 (2001)
doi:10.1006/jcat.2001.3339, available online at http://www.idealibrary.com on IDEAL®

Sulfur-Tolerant Pt-Supported Catalysts for Benzene Hydrogenation

II. Influence of Cation Exchange Level for Pt/MOR-Based Catalysts

L. J. Simon,*,† J. G. van Ommen,† A. Jentys,* and J. A. Lercher*,[1]

*Technische Universität München, Lehrstuhl für Technische Chemie II, Lichtenbergstrasse 4, D-85748 Garching, Germany; and †University of Twente, Faculty of Chemical Technology, Catalytic Processes and Materials, P.O. Box 217, 7500 AE Enschede, The Netherlands

Received March 28, 2001; revised July 4, 2001; accepted July 7, 2001

Two reaction pathways are described for the hydrogenation of benzene over Pt/MOR, i.e., (i) on the metal particles and (ii) on Brønsted acid sites of MOR at the boundary to the metal, with atomic hydrogen being dissociated on the metal. The ratio between the two pathways depends on the zeolite acid site concentration and on the available metal surface sites. The deactivation of fully H^+ ion exchanged zeolites and the markedly slower intrinsic rate on Na^+ ion exchanged samples led to a pronounced maximum in the steady-state activity for benzene hydrogenation with partly H^+ exchanged samples. At high pressure and in the presence of thiophene, the benzene hydrogenation activity of Pt/MOR was higher via the pathway involving Brønsted acid sites than via the pathway involving only Pt. Therefore, in the presence of thiophene the type of alkali cation exchanged did not significantly influence activity, whereas Brønsted acid site concentration did. The relative sulfur tolerance of Pt/MOR during benzene hydrogenation was shown to depend on (i) the acid site concentration, which increases both the benzene conversion and the rate of C–C bond breaking leading to coke formation, and (ii) the partial pressure of hydrogen, which increases the concentration of hydrogen atoms available for hydrogenating benzene molecules activated via both pathways. © 2001 Academic Press

INTRODUCTION

One of the major drawbacks of noble metal-based catalysts is their sensitivity toward sulfur under reducing conditions. For example, Pt–Re-based reforming catalysts cannot tolerate more than a few parts per million of sulfur compounds in the feed (1, 2). In general, the presence of acid sites enhances the sulfur tolerance of noble metal catalysts. This effect has been explained primarily by the electron deficiency of the metal induced *via* the metal–support interactions (3–7), which in turn is claimed to reduce the Pt–S bond strength.

Although several reviews reported that benzene hydrogenation occurs solely on the metal surface (8–10), the acidity of the support was also shown to positively influence the activity for aromatic hydrogenation reactions. Similarly to the increase in sulfur tolerance, this has been explained by an increase in Pt electron deficiency (7). Several authors (11–15) reported an enhancement in the activity of Pt and Pd for hydrogenation of aromatic molecules when supported on acidic carriers compared with catalysts on inert supports. In agreement with these authors, our study (16) on Pt supported on Na-MOR and K-LTL led us to conclude that in addition to the conventional benzene hydrogenation on the metal, a second pathway for the hydrogenation of benzene exists involving acid sites of the zeolite close to the metal. From the comparison of the kinetic behavior of Pt supported on variously acidic Na-MOR and K-LTL, it was concluded that benzene molecules were hydrogenated on both metal sites and Brønsted acid sites very close to the metal by hydrogen dissociated on the metal. It is interesting to note in this context that Pt supported on partially Brønsted acidic H/K-LTL catalyst was more active and stable for benzene hydrogenation in the absence and presence of 50 ppm thiophene than Pt supported on partially Brønsted acidic H/Na-MOR (both samples having similar acid site concentrations). The higher catalytic stability and sulfur tolerance of Pt-supported LTL catalysts have been attributed to the higher metal dispersion and higher proximity of metal and Brønsted acid sites compared with MOR.

Here, the effect of acid site concentration on the activity and sulfur tolerance of Pt supported on MOR for the hydrogenation of benzene in the absence and presence of thiophene is discussed. The type and exchange level of the alkali cations have been varied, and the effects of the alkali/H^+ ratio and hydrogen pressure on the main mechanism occurring under the experimental conditions used are described. Based on these results, a potential improvement of the sulfur tolerance of noble metal supported catalysts for aromatic hydrogenation is discussed.

[1] To whom correspondence should be addressed. Fax: +49 (0)89 28913544. E-mail: johannes.lercher@ch.tum.de.

0021-9517/01 $35.00
Copyright © 2001 by Academic Press
All rights of reproduction in any form reserved.

EXPERIMENTAL

Catalyst Preparation

Mordenites exchanged with Li^+, K^+, and Cs^+ were prepared from a commercial Na-mordenite sample (TOSOH, Si/Al = 9.0, Ref. HSZ-641NAA, Lot T960402). Twenty grams of the parent zeolite was exchanged three times for 3 h at 353 K with 500 ml of a solution of 0.033 M of cesium acetate (Aldrich), lithium acetate (Acros Organics), or potassium oxalate (Merck). After the samples were washed three times with 50 ml of deionized water the catalysts were dried at room temperature and calcined at 773 K for 3 h (heating rate of 2 K min^{-1}) in a flow of dry air of 40 ml min^{-1} per gram zeolite.

The NH_4^+ form of the mordenite was prepared by ion exchange of 20 g of the parent zeolite with a 0.1 M solution of NH_4NO_3 (Merck) at room temperature. The procedure was repeated three times and subsequently the samples were washed with 50 ml of deionized water and dried in air. H-MOR was obtained after calcination in dry air with a flow of 100 ml min^{-1} per gram zeolite at 723 K for 3 h at a heating rate of 5 K min^{-1}.

The zeolites were loaded with Pt applying liquid-phase ion exchange at room temperature using tetraammine platinum hydroxide ($Pt(NH_3)_4(OH)_2 \cdot H_2O$, 59% Pt, STREM) as precursor (17). The volume of the Pt precursor solution required to obtain a platinum loading of 1 wt% was added dropwise at a rate of 12 ml min^{-1} to the zeolite suspended in deionized water. The solution containing the zeolite and the precursor was stirred overnight. The catalyst was filtered, washed with deionized water, dried for 24 h in air at room temperature, calcined in a flow of air of 40 ml min^{-1} per gram catalyst at 493 K for 2 h (heating rate of 0.5 K min^{-1}), and finally reduced with hydrogen in a flow of 35 ml min^{-1} per gram catalyst at 623 K for 1 h (heating rate 0.5 K min^{-1}).

The samples are designated in this paper by Pt/XH-MOR, with X being the type of alkali cations and Pt/NH_4-MOR for the sample where all protons are exchanged with NH_4^+.

Pt/Na-MOR and Pt/K-MOR were prepared by ion exchange of the reduced Pt/XH-MOR (X = Na^+ and K^+) with sodium nitrate (Aldrich) and potassium nitrate (Merck), respectively, to exchange the protons formed during the decomposition and reduction of the Pt ions.

Catalyst Characterization

The chemical composition of the catalysts was determined by X-ray fluorescence spectroscopy. The concentration of strong acid sites was measured by ammonia temperature-programmed desorption (TPD). For this experiment, 90 mg of the sample was evacuated at 623 K for 1 h (heating rate of 10 K min^{-1}). After cooling to room temperature ammonia was adsorbed for 1 h with a partial pressure of 10 mbar. Physisorbed ammonia was removed by heating the sample *in vacuum* to 423 K for 1 h. TPD was performed up to 973 K with a heating rate of 10 K min^{-1}. A mass spectrometer was used to detect the desorbing molecules.

The number of accessible Pt atoms was determined from a hydrogen chemisorption isotherm. The catalyst was reduced in flowing hydrogen (flow rate approximately 50 ml min^{-1}) for 1 h at 623 K and subsequently evacuated (pressure $< 1.10^{-5}$ mbar) at this temperature for 1 h. After the sample was cooled to room temperature, 500 mbar of hydrogen was admitted into the sample chamber and allowed to equilibrate with the catalyst overnight. The sorption isotherm was measured with decreasing hydrogen pressure in steps applying equilibrium times of 1 h for each step.

X-Ray absorption spectra were collected on beamline X23A2 at NSLS, Brookhaven, New York, and on beamline X1 at HASYLAB, DESY, Hamburg, Germany. The storage rings were operated with an average current of 100 mA and electron energies of 2.5 GeV (NSLS) and 4.5 GeV (DESY). The Si(311) double-crystal monochromator used was detuned to 60% of the maximum intensity to minimize the intensity of higher harmonics in the X-ray beam. Data were collected at the Pt L_{III} edge (11564 eV) and analyzed with the WINXAS97 software (18).

For the EXAFS analysis the scattering contributions of the background were removed from the X-ray absorption spectra with two second-order polynomial functions. The oscillations were weighted with k^2 and Fourier transformed within the limits $k = 3.5$ and 16 $Å^{-1}$. The Pt–Pt contributions of the first coordination shell were isolated from the Fourier transformed oscillations in the range $r = 1.5$–3.2 Å (not corrected for the phase shift) and analyzed using phase shift and amplitude functions determined from bulk Pt.

Benzene Hydrogenation Measurements

The hydrogenation of benzene in the presence and absence of thiophene was performed using two parallel fixed-bed reactors. One reactor was used for reactions in the absence and the other for reactions in the presence of thiophene. To avoid sulfur contamination of the catalyst, all lines leading to the reactors were entirely separated. Between 45 and 90 mg of catalyst was mixed with the same amount of quartz and reduced *in situ* in a hydrogen flow of 200 ml min^{-1} at 673 K for 1 h. A temperature of 623 K was chosen for the *in situ* reduction of Pt/NH_4-MOR where the decomposition of NH_4^+ in NH_3 and H^+ does not occur. The activity of the catalysts as a function of pressure was studied at 623 K with H_2/C_6H_6 ratios of 7.6 at 1 and 10 bar and 20.6 at 25 bar. A solution of benzene (Aldrich, 99.9%) and thiophene (Aldrich) was injected into the gas stream using a high-pressure single-piston pump (Isco). During all kinetic measurements in the presence of sulfur, the concentration of thiophene in the feed was always maintained at 50 ppm. The reaction products were analyzed using an

on-line HP6980 gas chromatograph with a FID detector and a DB-1 column. Product concentrations were calculated using calibration factors for each products and the rates of benzene hydrogenation were calculated using benzene conversion levels below 8.4%.

RESULTS

Characterization

The chemical and physicochemical properties of the catalysts are summarized in Table 1. The acid site concentrations determined by ammonia TPD were generally lower than the values determined theoretically from the chemical analysis. The loading of Pt led to a decrease in the concentration of acid sites, i.e., from 1.41 to 1.30 mmol g^{-1} for H-MOR and Pt/H-MOR, respectively. The Pt loading and dispersion of Pt inside the zeolite pores were similar for all catalysts prepared.

The results of the EXAFS analysis are compiled in Table 2. Pt–Pt coordination numbers above 8 obtained for the reduced samples are in good agreement with the moderate values of Pt dispersion obtained by hydrogen chemisorption. Although Pt–Pt coordination numbers were high, indicating that the diameter of the Pt particles was larger than the pores of MOR (approximately 2 nm), the tilting of the samples under the electron beam of a TEM showed that most of the Pt particles had grown inside the crystallites of MOR for Pt/H-MOR and Pt/NaH-MOR (16). The Pt–Pt interatomic distances varied between 2.74 and 2.77 Å for all catalysts. Clear changes in Pt–Pt interatomic distances due to the bonding of sulfur on the Pt surface were not observed. High Debye–Waller factors ($\Delta\sigma^2_{Pt-Pt}$) were observed for all catalysts, and did not significantly change after reaction. Only for Pt/H-MOR was the Pt–Pt coordination number affected by the presence of thiophene.

The area of the peak above the absorption edge in the XANES spectra of the reduced Pt samples was integrated after subtracting the continuum step from the fitted arctan function (19). The area of the Pt white line increased with increasing acid site concentration as shown in Fig. 1.

TABLE 2

Results of the EXAFS Analysis of the Catalysts before and after Benzene Hydrogenation in the Absence and Presence of 50 ppm Thiophene (623 K, 1 bar, $H_2/C_6H_6 = 34.2$)

Sample	State of the sample	N_{Pt-Pt}	R_{Pt-Pt} (Å)	$\Delta\sigma^2_{Pt-Pt}$ (Å^2)
Pt/H-MOR	H_2	9.3	2.77	1.3×10^{-3}
	$H_2 + C_6H_6$	9.1	2.76	3.1×10^{-3}
	$H_2 + C_6H_6 + C_4H_4S$	10.7	2.76	2.3×10^{-3}
Pt/NaH-MOR	H_2	9.0	2.75	4.0×10^{-3}
	$H_2 + C_6H_6$	10.7	2.75	4.6×10^{-3}
	$H_2 + C_6H_6 + C_4H_4S$	10.5	2.75	4.4×10^{-3}
Pt/LiH-MOR	H_2	8.6	2.74	5.3×10^{-3}
	$H_2 + C_6H_6$	9.9	2.75	5.6×10^{-3}
	$H_2 + C_6H_6 + C_4H_4S$	9.9	2.74	6.5×10^{-3}
Pt/KH-MOR	H_2	9.6	2.76	3.1×10^{-3}
	$H_2 + C_6H_6$	9.8	2.75	2.5×10^{-3}
	$H_2 + C_6H_6 + C_4H_4S$	9.6	2.76	3.5×10^{-3}
Pt/CsH-MOR	H_2	8.2	2.76	3.2×10^{-3}
	$H_2 + C_6H_6$	8.4	2.75	2.3×10^{-3}
	$H_2 + C_6H_6 + C_4H_4S$	8.4	2.75	2.9×10^{-3}

Influence of Pressure and Presence of Thiophene on Benzene Hydrogenation

The activity of the catalysts for benzene hydrogenation was measured at 1, 10, and 25 bar in the absence and presence of 50 ppm thiophene. The catalyst activity for benzene hydrogenation, shown at 10 bar in Fig. 2, was stable after 30 min TOS in the absence and presence of 50 ppm thiophene for all catalysts. Rates of benzene hydrogenation after 1 h TOS in the absence and presence of 50 ppm thiophene are compiled in Table 3. In all cases Pt/XH-MOR samples showed higher activity than Pt/H-MOR, while Pt/NH_4-MOR, Pt/Na-MOR, and Pt/K-MOR were

TABLE 1

Chemical and Physicochemical Characterizations of the Samples

Sample	Formula	Acid sites (mmol g^{-1})		BET surface area (m^2 g^{-1})	Pt (wt%)	H/Pt
		Theoretical	Experimental			
Na-MOR	$Na_{4.8}(Al_{4.8}Si_{43.2}O_{96}) \cdot 24H_2O$	—	—	323	—	—
H-MOR	$Na_{0.1}H_{4.7}(Al_{4.8}Si_{43.1}O_{96}) \cdot 24H_2O$	1.65	1.41	324	—	—
Pt/H-MOR	$Na_{0.1}H_{4.6}(Al_{4.8}Si_{43.2}O_{96}) \cdot 24H_2O$	1.61	1.30	321	1.13	0.56
Pt/NH_4-MOR	$Na_{0.1}(NH_4)_{4.6}(Al_{4.8}Si_{43.2}O_{96}) \cdot 24H_2O$	1.62	(1.42)[a]	284	1.10	0.58
Pt/LiH-MOR	$Li_{2.7}H_{2.1}(Al_{4.8}Si_{43.1}O_{96}) \cdot 24H_2O$	0.74	0.74	318	0.95	0.62
Pt/NaH-MOR	$Na_{3.4}H_{1.4}(Al_{4.7}Si_{43.2}O_{96}) \cdot 24H_2O$	0.47	0.26	307	1.10	0.59
Pt/KH-MOR	$K_{4.4}H_{0.4}(Al_{4.8}Si_{43.1}O_{96}) \cdot 24H_2O$	0.13	0.10	311	0.99	0.51
Pt/CsH-MOR	$Cs_{4.1}H_{0.7}(Al_{4.8}Si_{43.1}O_{96}) \cdot 24H_2O$	0.20	0.19	287	1.01	0.52
Pt/Na-MOR	$Na_{4.7}H_{0.1}(Al_{4.8}Si_{43.2}O_{96}) \cdot 24H_2O$	0.03	0.09	296	0.96	0.58
Pt/K-MOR	$K_{4.8}(Al_{4.8}Si_{43.1}O_{96}) \cdot 24H_2O$	0	0.03	303	1.09	0.56

[a] The acid sites are covered by ammonium cations and, thus, not available for the reaction.

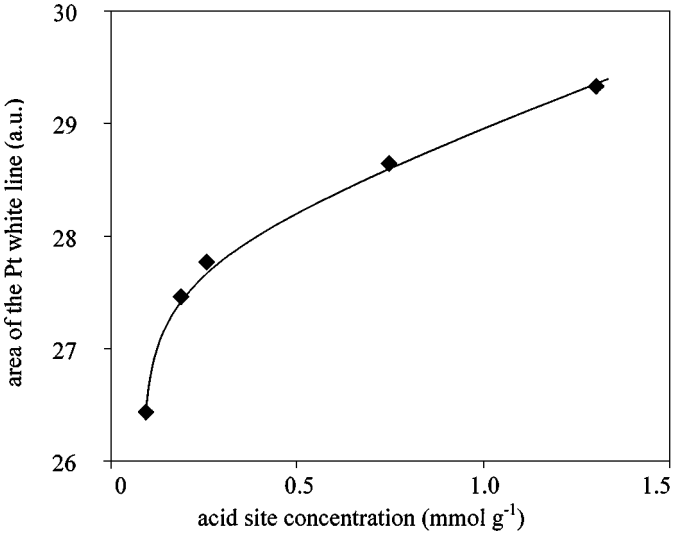

FIG. 1. Correlation between acid site concentration and Pt white line area for reduced Pt supported on partially exchanged MOR.

significantly less active. The ratios between benzene hydrogenation rates in the absence and presence of 50 ppm thiophene (r/r_s) are reported in Table 4. At 1 bar significantly higher r/r_s ratios were observed for Pt/H-MOR than for partially alkali exchanged Pt/XH-MOR catalysts. The increase in the total pressure to 10 bar (at a constant benzene/hydrogen ratio) led to an increase in the r/r_s ratio for all catalysts, indicating higher deactivation of the catalysts in the presence of thiophene compared with that at 1 bar. Similar to the reaction at 1 bar, the r/r_s ratio observed for Pt/H-MOR was higher than for Pt/XH-MOR catalysts. When the hydrogen partial pressure was increased to 25 bar the r/r_s ratio stayed constant or decreased for samples having an acid site concentration higher than 0.26 mmol g^{-1}, indicating a lower deactivation compared with experiments at lower pressures. The r/r_s ratios observed for Pt/LiH-MOR and Pt/KH-MOR at 25 bar hydrogen partial pressure were higher than those for Pt/H-MOR and Pt/NaH-MOR (Table 4).

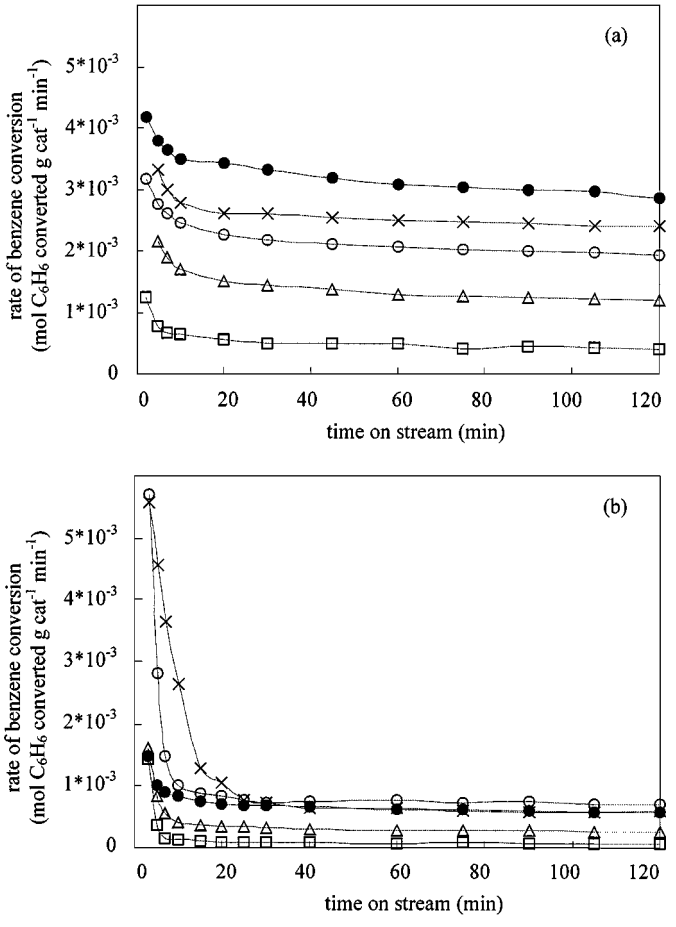

FIG. 2. Benzene hydrogenation (10 bar, 623 K, $H_2/C_6H_6 = 7.6$) in the absence (a) and presence (b) of 50 ppm thiophene for (□) Pt/H-MOR, (○) Pt/LiH-MOR, (×) Pt/NaH-MOR, (△) Pt/KH-MOR, and (●) Pt/CsH-MOR.

Influence of Acid Site Concentration on Benzene Hydrogenation

The influence of acid site concentration on the rate of benzene hydrogenation is shown in Fig. 3. In general, the

TABLE 3

Rate of Benzene Conversion (moles of benzene converted per gram catalyst per minute) after 1 h TOS (623 K) at 1 bar and 10 bar ($H_2/C_6H_6 = 7.6$) and 25 bar ($H_2/C_6H_6 = 20.3$) in the Absence of Thiophene (r) and Presence of 50 ppm Thiophene (r_s)

Catalyst	1 bar		10 bar		25 bar	
	r	r_s	r	r_s	r	r_s
Pt/H-MOR	6.8×10^{-5}	2.0×10^{-5}	4.9×10^{-4}	7.5×10^{-5}	1.2×10^{-3}	5.5×10^{-4}
Pt/NH_4-MOR	—	—	—	—	5.1×10^{-4}	2.1×10^{-5}
Pt/LiH-MOR	1.4×10^{-4}	9.3×10^{-5}	2.1×10^{-3}	7.7×10^{-4}	1.2×10^{-2}	4.1×10^{-3}
Pt/NaH-MOR	1.6×10^{-4}	9.9×10^{-5}	2.5×10^{-3}	6.5×10^{-4}	6.8×10^{-3}	5.0×10^{-3}
Pt/KH-MOR	8.6×10^{-5}	5.2×10^{-5}	1.2×10^{-3}	3.4×10^{-4}	5.9×10^{-3}	1.2×10^{-3}
Pt/CsH-MOR	1.4×10^{-4}	1.0×10^{-4}	2.5×10^{-3}	6.3×10^{-4}	—	—
Pt/K-MOR	—	—	—	—	6.2×10^{-4}	5.1×10^{-5}
Pt/Na-MOR	—	—	—	—	5.7×10^{-3}	3.3×10^{-4}

TABLE 4

Ratio between Benzene Hydrogenation Rates in the Absence of Thiophene (r) and the Presence of 50 ppm Thiophene (r_s) after 1 h TOS at 1, 10, and 25 bar (623 K)

	1 bar	10 bar	25 bar
Pt/H-MOR	3.3	6.5	2.2
Pt/NH_4-MOR	—	—	24.3
Pt/LiH-MOR	1.5	2.7	2.8
Pt/NaH-MOR	1.6	3.9	1.4
Pt/KH-MOR	1.7	3.7	5.1
Pt/CsH-MOR	1.3	3.9	—
Pt/K-MOR	—	—	12.0
Pt/Na-MOR	—	—	17.3

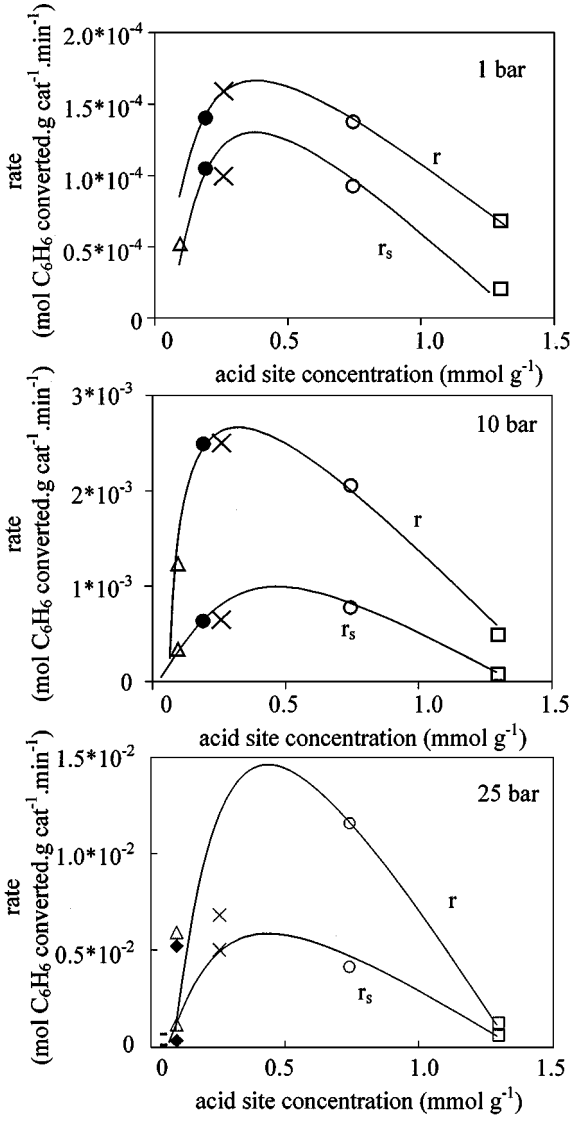

FIG. 3. Relation between acid site concentration and rate of benzene conversion after 1 h TOS in the absence (r) and presence (r_s) of 50 ppm thiophene for (□) Pt/H-MOR, (○) Pt/LiH-MOR, (×) Pt/NaH-MOR, (△) Pt/KH-MOR, (●) Pt/CsH-MOR, (▬) Pt/K-MOR, and (◆) Pt/Na-MOR (623 K, $H_2/C_6H_6 = 7.6$ at 1 and 10 bar and 20.3 at 25 bar).

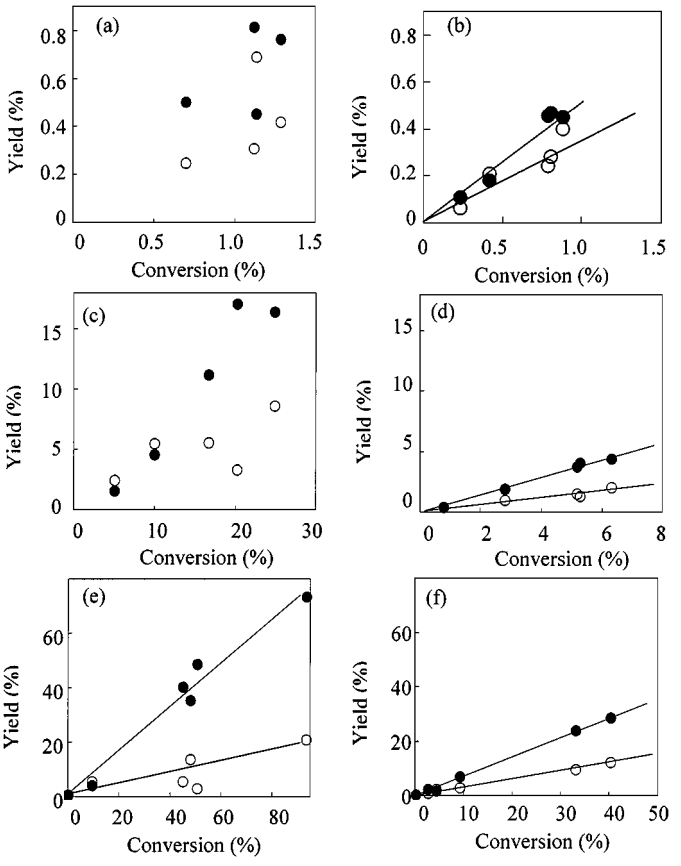

FIG. 4. Effect of benzene conversion on yields of (●) cyclohexane and (○) methylcyclopentane for Pt/NaH-MOR at (a) 1 bar, (b) 1 bar in the presence of 50 ppm thiophene, (c) 10 bar, (d) 10 bar in the presence of 50 ppm thiophene, (e) 25 bar, and (f) 25 bar in the presence of 50 ppm thiophene (623 K).

rate of benzene hydrogenation increased for all atalysts with increasing pressure from 1 to 25 bar. For all pressures, hydrogenation activity showed an optimum concentration of acid sites around 0.5 mmol g^{-1}. In the presence of 50 ppm thiophene, the rates of hydrogenation decreased for all catalysts, but the optimum in activity was still observed at all pressures studied.

Product Formation on Pt/NaH-MOR

The yields of cyclohexane and methylcyclopentane at 1, 10, and 25 bar in the absence and presence of 50 ppm thiophene as function of the conversion are shown in Fig. 4. At 1 and 10 bar in the absence of thiophene a clear relation between benzene conversion and the yields of cyclohexane and methylcyclopentane was not observed (Fig. 4). In contrast, in the presence of thiophene the yields of product formation were always a linear function of the conversion (Figs. 4b, 4d, and 4e). The positive slope at the origin indicates that both cyclohexane and methylcyclopentane were primary products of the benzene hydrogenation reaction in the presence of thiophene.

DISCUSSION

Support Effects

The MOR structure is based on two independent monodimensional channel systems with openings of 2.6×5.7 Å (8-membered rings) and 6.5×7.0 Å (12-membered rings, main channels with side pockets) (20). Benzene and cyclohexane (kinetic diameter around 5.8 Å) have been shown not to be able to enter the 8-membered ring channels of MOR (21–23). Therefore, the locations of the acid sites, the alkali cations, and Pt play an important role in the catalytic properties of MOR for benzene hydrogenation. Two of the five ion exchangeable sites of MOR, i.e., sites I and I′, are located in 8-membered ring channels, while the other sites are located in side pockets and main channels of MOR (24). The small size of alkali cations allows ion exchange at sites in both channel systems of MOR. In the case of H-MOR, which was prepared from the Na-MOR before metal ion exchange, a fraction of the Brønsted acid sites measured by NH_3 TPD (Table 1) is located in the 8-membered ring channels and is, therefore, not available for the reaction. However, the protons formed by decomposition of the Pt precursor are located only in the main channel as $(Pt(NH_3)_4)^{2+}$ cations are too big to enter the 8-membered ring. This implies that Brønsted acid sites formed after decomposition of the Pt precursor are in close vicinity of the metal.

The Pt white line intensity increased with increasing acid site concentration and reached a maximum value (Fig. 1), which suggests that changes in acid site concentration influence the metal electronic properties. Several models have been proposed to explain these variations. One model attributes the increase in metal electron density with increasing alkali content in zeolites to the higher electron donation of lattice oxygens to the metal (7, 25). In contrast, Sachtler and co-workers (26, 27) proposed the "proton adduct" model, where the zeolite protons are delocalized on the metal and, thus, attract electrons from the metal clusters. Both models imply an electron transfer from lattice oxygens to metal clusters or from the metal clusters to protons. More recently, Mojet *et al*. (28) suggested that changes in metal electronic properties were not due to electron transfer, but that the effects resulted from the decrease in metal particle ionization potential induced by the electrostatic Coulomb potential of the support in the presence of alkali cations. For the catalysts prepared from alkali zeolites (all samples except Pt/H-MOR and Pt/NH_4-MOR), protons formed by decomposition of the Pt precursor are located in the main channels and side pockets of MOR and, therefore, are in close contact to the Pt particles. Consequently, interactions between the metal and the Brønsted acid sites may occur. With decreasing acid site concentration, the average distance between the metal clusters and the protons increases and less influence on metal electronic properties is observed.

Significant changes in Si/Al ratios after Pt ion exchange were not observed, indicating that the integrity of the samples remains intact throughout all preparation treatments. The lower acid site concentration observed for Pt/H-MOR compared with H-MOR, i.e., 1.4 and 1.3 mmol g^{-1}, respectively, and the small decrease in BET surface area suggest that a small fraction of acid sites is inaccessible after Pt loading in MOR. The differences between theoretical and experimental acid site concentration decreases with decreasing acid site concentration of the samples, indicating that a larger number of acid sites are shielded by the metal particles for highly acidic samples. For instance, assuming that metal particles consist of 250 atoms and that four protons are shielded per metal cluster, 0.32 mmol g^{-1} of H^+ will be affected. Subtracting this value from the theoretical acid site concentration for Pt/H-MOR (Table 1), reveals that the theoretical and experimental acid site concentrations are in good agreement. Therefore, the decrease in acid site concentration after loading of Pt can be attributed to the shielding of a portion of the acid sites by metal particles.

Characterization of the Metal Particles

A good correlation was observed between the average Pt particle sizes estimated by EXAFS (Table 2), hydrogen chemisorption (Table 1), and HREM (16). Rather large Pt clusters with an average particle size of 2 nm were found to be located inside the pores of MOR. We speculate that metal particles grew and were blocked inside the pores, inducing local defects during calcination and reduction treatments. This is consistent with the small decrease in peak intensity in XRD patterns observed in the presence of Pt. Note that the size of the Pt particles is in good agreement with results reported by Reifsnyder *et al*. (29), who observed the presence of 2-nm Pd clusters inside the MOR lattice also creating local defects. Additional evidence for the location of the particles comes from the high value of the Debye–Waller factor, as Jentys *et al*. (30) showed that higher Debye–Waller factors are generally characteristic of Pt located inside zeolite pores.

Mechanism of Benzene Hydrogenation

Benzene hydrogenation has generally been described as a monofunctional reaction on metals (8–10). The reaction was shown to occur via three subsequent hydrogenation steps, which finally led to the formation of cyclohexane. In the presence of acid sites, isomerization to methylcyclopentane occurs as a parallel and secondary reaction, if cyclohexene can desorb from the metal particle.

The increase in the support acidity has been shown to increase catalytic activity for benzene hydrogenation (4, 7). This has been explained by the decrease in the apparent electron density of the metal with increasing acid site concentration, which favors the adsorption of aromatic

molecules. In agreement with this model, the Pt white line intensity in the XANES increased with increasing acid site concentration, which suggests a decrease in the metal apparent electron density. If this is the only route to enhance the reaction rate, the activity increase should vary sympathetically with the Brønsted acid site concentration. In contrast to this model, however, we observed an optimal acid site concentration with respect to catalyst activity (see Fig. 3). Thus, in agreement with previous suggestions of two principal hydrogenation routes on supported metal catalysts (11–15), we propose that Brønsted acid sites are directly involved in the reaction pathway during benzene hydrogenation. Our previous work (16) showed that Pt supported on partially sodium exchanged MOR and potassium exchanged LTL were more active and sulfur resistant for benzene hydrogenation than more acidic and more basic catalysts. The higher activity and sulfur resistance of Pt/KH-LTL compared with Pt/NaH-MOR were explained by the close vicinity of the metal and Brønsted acid sites for the former sample (16). It is concluded that in addition to the metal catalyzed route (route A), a reaction route on Brønsted acid sites (route B) exists as schematically depicted in Fig. 5. In route B, benzyl carbenium ions are formed in the vicinity or at the perimeter of the Pt particles and are hydrogenated with hydrogen atoms dissociated on the metal surface.

At 25 bar and in the presence of thiophene, the correlation observed between the yields of cyclohexane and benzene conversion for Pt/NaH-MOR (Fig. 4) shows that cyclohexane and methylcyclopentane are primary products. Note that in route B methylcyclopentane and cyclohexane are formed on Brønsted acid sites from the same reaction intermediate, i.e., a cyclohexyl carbonium ion, and, therefore, both must be primary reaction products (31). In route A, in contrast, cyclohexane is formed as primary product and a significant fraction is further isomerized after dehydrogenation on the metal surface to cyclohexene on the Brønsted acid sites to methylcyclopentene. In the final step, methylcyclopentene is hydrogenated again on the metal surface to form methylcyclopentane. The formation of methylcyclopentane depends, then, on the concentration of cyclohexane formed and is conceptually a secondary product of the reaction. However, neither cyclohexene nor methylcyclopentene was detected during the reactions, which indicates that they occur only in small concentrations and only inside the zeolite pores.

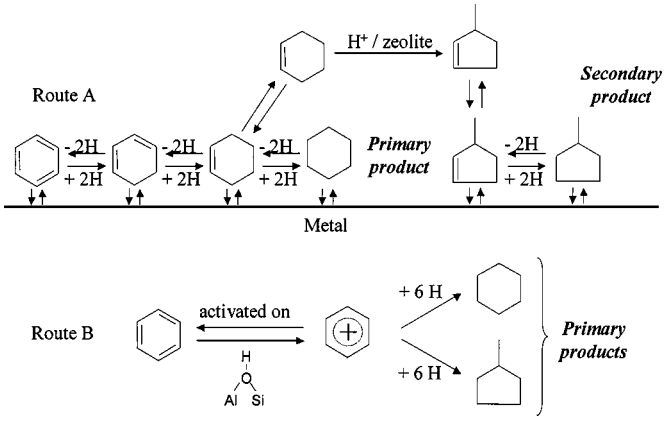

FIG. 5. Two routes of benzene hydrogenation on Pt-supported MOR, i.e., route A on the metal and route B on Brønsted acid sites with hydrogen dissociated on the close metal surface.

Metal electronic properties during benzene hydrogenation in the absence and presence of thiophene have previously been studied using *in situ* XANES on Pt/Na-MOR, Pt/NaH-MOR, and Pt/H-MOR (32). A decrease in Pt white line intensity during benzene hydrogenation indicated that the sorption of benzene molecules via π electrons influenced the metal electron properties. The same study showed that during benzene hydrogenation in the presence of thiophene, Pt white line intensity increased, which was attributed to the irreversible sorption of sulfur species on the metal surface. The study of thiophene poisoning of the metal surface showed that an equilibrium between the surface sulfur species and thiophene in the gas phase exists and that the metal surface is not fully sulfur poisoned under the reaction conditions. Therefore, we concluded that in the presence of thiophene, the sorption of benzene molecules was strongly reduced, significantly suppressing the benzene hydrogenation activity to cyclohexane of the metal (Figs. 4b, 4d, 4f). As the catalysts are still active in the presence of thiophene and as Pt/NaH-MOR was more active compared with Pt/Na-MOR and Pt/H-MOR, we concluded that, while hydrogenation is reduced on the metal (route A), sorption and decomposition of hydrogen molecules on Pt in the presence of thiophene are still possible, thus keeping the hydrogenation properties of the catalysts via route B.

It is important to note that a significantly lower rate of benzene hydrogenation was also observed for Pt/NH_4-MOR compared with other catalysts. This is attributed to the absence of Brønsted acid sites in this material, which therefore, similarly to the Pt/X-MOR catalysts, converted benzene only on the Pt surface (see Table 3). The low activity of Pt/NH_4-MOR, Pt/Na-MOR, and Pt/K-MOR catalysts compared with the acid site-containing catalysts (Pt/H-MOR and Pt/XH-MOR) and the previously reported XANES study (32) led us to conclude that in the presence of sulfur, the hydrogenation rate of benzene on Pt supported MOR is significantly higher via route B than via route A. Note that the rates of benzene hydrogenation in the absence of thiophene were similar for Pt/NH_4-MOR and Pt/K-MOR, while the rate was lower for Pt/NH_4-MOR in the presence of thiophene. As benzene is converted only on the metal on these two samples, this suggests that potassium has a more positive effect on the activity of the metal than ammonium cations.

Effect of Reactant Pressure

In the absence of thiophene the increase in pressure from 1 to 10 bar ($H_2/C_6H_6 = 7.6$) and 25 bar ($H_2/C_6H_6 = 20.3$) increased benzene hydrogenation rates (see Fig. 3), which is attributed to a higher surface concentration of reactant molecules on the catalyst.

The higher r/r_s ratio at 10 bar indicates that the decrease in benzene hydrogenation rates is higher in the presence of thiophene at 10 bar compared with 1 bar. The increase in thiophene partial pressure increased catalyst sulfur poisoning, i.e., possibly by increasing metal sulfur poisoning and coke formation. Consequently, both sites were affected by the presence of thiophene. But due to the similarity of the changes in r/r_s ratio at 1 and 10 bar for all catalysts, i.e., a factor 2 higher at 10 bar compared with 1 bar, we speculate that the deactivation is caused mainly by metal site sulfur poisoning and not by the blocking of Brønsted acid sites by coke deactivation. We therefore concluded that the presence of thiophene at 10 bar strongly reduced the activity on the metal and, thus, the reaction via route A, while the activity on Brønsted acid sites was less affected (see Fig. 2 and Table 3) and, consequently, was still available as benzene anchors on Brønsted acid sites in the reaction scheme for benzene hydrogenation.

The increase in hydrogen partial pressure from 10 to 25 bar increased (i) hydrogen dissociation on the metal surface and, thus, increased the concentration of hydrogen available for benzene hydrogenation via both routes (Table 3), and (ii) the H_2/H_2S ratio, thus decreasing the metal sulfur poisoning for catalysts forming more H_2S, i.e., catalysts having a medium or high acid site concentration (33).

The higher r/r_s ratio observed for Pt/H-MOR compared with Pt/XH-MOR at 1 and 10 bar is attributed to the higher formation of H_2S by thiophene decomposition on Brønsted acid sites, increasing the probability of metal sulfur poisoning (32).

Sulfur Tolerance of Pt-Supported MOR: A Matter of Acid Site Concentration?

Generally, sulfur-tolerant Pt-supported catalysts for hydrogenation reactions are based on more acidic supports, as shown by several industrial applications (34–36). The effect of support acidity on the kinetic behavior of the catalysts has been often explained by changes in electronic properties of Pt (5). However, our study clearly showed that, in contrast to the previous reports, a catalyst having a medium acid site concentration is more sulfur tolerant for benzene hydrogenation than one with a high acid site concentration. The changes in catalytic activity in the absence and presence of thiophene, i.e., the differences in deactivation between Pt/NaH-MOR and Pt/H-MOR at low and high pressure, cannot be attributed solely to coke formation and blocking of metal sites by sulfur.

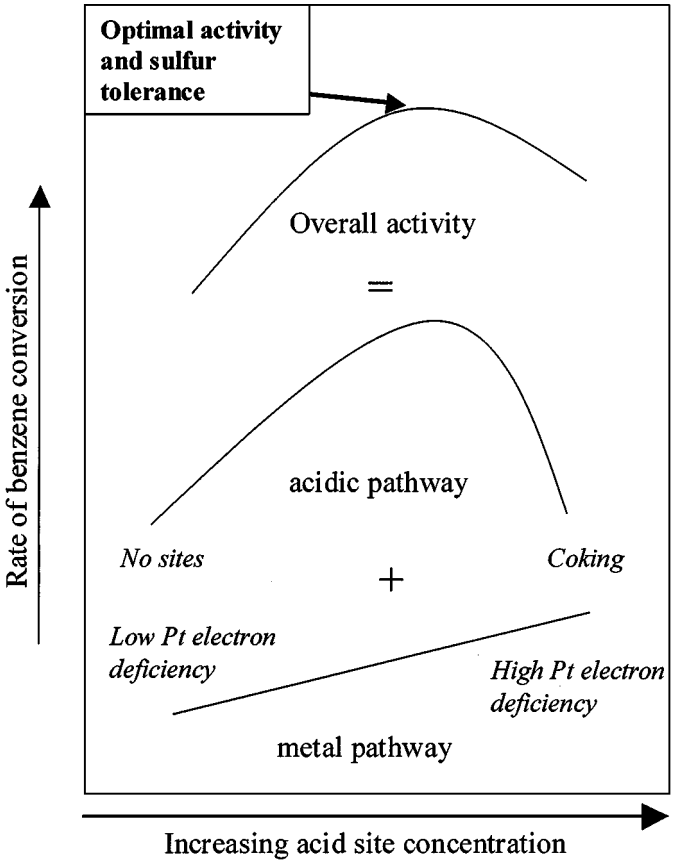

FIG. 6. Schematic presentation of the overall activity of the catalysts versus concentration of acid sites expected from the two pathways of benzene hydrogenation.

The two routes described for benzene hydrogenation on Pt-supported MOR suggest a new way to improve noble metal sulfur tolerance in the hydrogenation of aromatic molecules. A model of the overall activity with increasing concentration for the two pathways of benzene hydrogenation is shown in Fig. 6. For route A, the metal only catalyzed reaction route, the type of cation is theoretically expected to influence the activity by changing the electronic properties of Pt (7). For the acid catalyzed pathway, in contrast, the type of counterion should have no effect on the activity, as the presence of sulfur mainly affects the activity of the metal surface.

The results reported here lead to conclusion that changes in the electronic properties of Pt caused by changing the type of alkali cation have only a minor effect on hydrogenation activity in the presence of sulfur, i.e., when the metal surface is sulfur poisoned, while the alkali exchange level has a major influence on catalytic behavior. A low acid site concentration, i.e., by exchanging protons with alkali or ammonium cations, resulted in low-activity catalysts in the presence of thiophene, which could not hydrogenate benzene molecules via route B. The other extreme, a very high Brønsted acid site concentration, leads to a higher

deactivation by coking (37), which is formed from the unsaturated molecules resulting from the decomposition and polymerization of benzene and thiophene molecules on Brønsted acid sites. Therefore, to achieve optimum benzene hydrogenation activity and sulfur tolerance, noble metal-based zeolite catalysts should contain an intermediate concentration of acid site, which is sufficient to hydrogenate aromatic molecules and does not significantly deactivate the catalytic activity by coke formation. The location and proximity of metal and Brønsted acid sites (presumably these sites are located on the perimeter of the metal particle) play a significant role and can be optimized.

CONCLUSIONS

Benzene hydrogenation on Pt-supported MOR has been found to occur via two pathways: (i) hydrogenation on the metal surface only, and (ii) hydrogenation on acid sites close to Pt particles with hydrogen dissociated on the Pt. An optimal acid site concentration is required to achieve an optimal benzene hydrogenation activity. In the presence of thiophene, the benzene hydrogenation activity on the acid sites (route B) was significantly higher than the activity of the metal surface (route A). Therefore, the type of alkali cation did not have a strong influence on the benzene hydrogenation activity of Pt supported on MOR. An increase in hydrogen partial pressure increases the sulfur tolerance of the catalysts by decreasing the poisoning of the metal surface and favoring the hydrogenation of benzene on the Brønsted acid sites using hydrogen dissociated on the metal surface. The balance between acid sites and available metal sites has been best met for Pt/NaH-MOR. The model proposed here, i.e., to increase the sulfur tolerance of Pt by adjusting the Brønsted acid site concentration of the support to an optimum value, while increasing the hydrogen partial pressure to increase the decomposition of hydrogen on the metal surface, can be applied to a wide variety of macroporous and microporous supports that are more active for aromatic hydrogenation. It thus has the potential to lead to a highly active and sulfur-resistant catalyst.

ACKNOWLEDGMENTS

This work was supported by STW/NWO, The Netherlands, under Project 349-3787 and has been performed under the auspices of NIOK and PIT.

XAFS experiments were carried out at X1, HASYLAB, DESY, Hamburg, Germany, which is supported by TMR Contract ERBFMGECT950059 of the European Community, and at the National Synchrotron Light Source, Brookhaven National Laboratory, Brookhaven, New York, which is supported by the U.S. Department of Energy, Division of Materials Sciences and Division of Chemical Sciences under Contract DE-AC02-98CH10886.

REFERENCES

1. Menon, P. G., and Prasad, J., *in* "Proceedings, 6th International Congress on Catalysis" (G. C. Bond et al., Eds.), London, Vol. 2, p. 1061, 1977.
2. Franck, J. P., and Martino, G. P., *in* "Deactivation and Poisoning of Catalysts" (J. Oudar and W. Wise, Eds.), p. 205. Dekker, New York, 1985.
3. Landau, M. V., Kruglikov, V. Y., Goncharova, N. V., Konoval'chikov, O. D., Chukin, G. D., Smirnov, B. V., and Malevich, V. I., *Kinet. Catal.* **17**, 1104 (1976).
4. Frety, R., Da Silva, P. N., and Guenin, M., *Catal. Lett.* **3**, 9 (1989).
5. Marecot, P., Mahoungou, and J. R., Barbier, J., *Appl. Catal. A* **101**, 143 (1993).
6. Miller, J. T., and Koningsberger, D. C., *J. Catal.* **162**, 209 (1996).
7. de Mallman, A., and Barthomeuf, D., *J. Chim. Phys.* **87**, 535 (1990).
8. Smith, H. A., *in* "Catalysis," Vol. V: "Hydrogenation" (P. H. Emmett, Ed.). Reinhold, New York, 1957.
9. Bond, G. C., "Catalysis by Minerals," Academic Press, New York/London, 1962.
10. Stanislaus, A., and Cooper, B. H., *Catal. Rev. Sci. Eng.* **36**, 75 (1994).
11. Chou, P., and Vannice, M. A., *J. Catal.* **107**, 129 (1987).
12. Lin, S. D., and Vannice, M. A., *J. Catal.* **143**, 539 (1993).
13. Lin, S. D., and Vannice, M. A., *J. Catal.* **143**, 554 (1993).
14. Lin, S. D., and Vannice, M. A., *J. Catal.* **143**, 563 (1993).
15. Wang, J., Huang, L., and Li, Q., *Appl. Catal. A* **175**, 191 (1998).
16. Simon, L. J., van Ommen, J. G., Jentys. A., and Lercher, J. A., *J. Catal.* **201**, 60 (2001), doi:10.1006/jcat.2001.3236.
17. Jentys, A., Englisch, M., Haller, G. L., and Lercher, J. A., *Catal. Lett.* **21**, 303 (1993).
18. Ressler, T., *J. Phys. IV* **C2**, 7 (1997).
19. Outka, D. A., and Stöhr, J., *J. Phys. Chem.* **94**, 8621 (1990).
20. Meier, W. M., Olson, D. H., and Baerlocher, Ch., "Atlas of Zeolite Structure types." Elsevier, Amsterdam, 1996.
21. Barrer, R. M., and Peterson, D. L., *Proc. R. Soc. Lond. Ser. A* **280**, 466 (1964).
22. Karge, H. G., *in* "Molecular Sieves—2, 4th International Conference" (J. R. Katzer, Ed.), ACS symp. Ser. 40, p. 584. Am. Chem. Soc., Washington, DC, 1977.
23. Mishin, I. V., Plakhotnik, V. A., Kasputin, G. I., Klyachko, A. L., and Slinkin, A. A., *Kinet. Catal.* **24**, 1448. (1983).
24. Schlenker, J. L., Pluth, J. J., and Smith, J. V., *Mater. Res. Bull.* **14**, 751 (1979).
25. Larsen, G., and Haller, G. L., *Catal. Lett.* **3**, 103 (1989).
26. Sheu, L. L., Knözinger, H., and Sachtler, W. M. H., *Catal. Lett.* **2**, 129 (1989).
27. Sheu, L. L., Knözinger, H., and Sachtler, W. M. H., *J. Am. Chem. Soc.* **111**, 8125 (1989).
28. Mojet, B. L., Miller, J. T., Ramaker, and D. E., Koningsberger, D. C., *J. Catal.* **186**, 373 (1999).
29. Reifsnyder, S. N., Otten, M. M., and Lamb, H. H., *Catal. Today* **39**, 317 (1998).
30. Jentys, A., Simon, L. J., and Lercher, J. A., *J. Phys. Chem. B* **104**, 9411 (2000).
31. Wang, J., Li, Q., and Yao, J., *Appl. Catal. A* **184**, 181 (1999).
32. Simon, L. J., van Ommen, J. G., Jentys, A., and Lercher, J. A., *J. Phys. Chem. B* **104**, 11644 (2000).
33. Guenin, M., Breysse, M., Frety, R., Tifouti, K., Marecot, P., and Barbier, J., *J. Catal.* **105**, 144 (1987).
34. Haun, E. C., Thompson, G. J., Gorawa, J. K., and Sullivan, D. K., U.S. Patent 5,114,562 (1992).
35. Schweizer, A. E., U.S. Patent 4,992,617 (1991).
36. Dessau, R. E. U.S. Patent 5,103,066 (1992).
37. Fouche, V., Magnoux, P., and Guisnet, M., *Appl. Catal.* **58**, 189 (1990).